

Low-temperature optical and transport properties of $\text{Hg}_{1-x}\text{Mn}_x\text{Se}$ single crystals

O Žižić†, Z V Popović‡, V A Kulbachinskii§ and A Milutinović‡

†Faculty of Mechanical Engineering, University of Belgrade, Yugoslavia

‡Institute of Physics, PO Box 57, 11000 Belgrade, Yugoslavia

§Department of Physics, Moscow State University, 117234 Moscow, Russia

Received 9 September 1991, in final form 23 June 1992, accepted for publication 14 July 1992

Abstract. The optical and transport properties of semimagnetic semiconductor $\text{Hg}_{0.86}\text{Mn}_{0.14}\text{Se}$ in the temperature range 10–300 K have been studied. The far-infrared reflectivity spectra of this alloy were analysed using a numerical fitting procedure, based on the model of plasmon–phonon interaction. The characteristic frequencies of the phonons and plasmons and their temperature dependences were determined. The electron concentration, as defined by the Hall and Shubnikov–de Haas effect, practically does not depend on the temperature or on the applied magnetic field. By combining the results of the optical and transport measurements, the temperature dependences of effective mass and carrier mobility were determined.

1 Introduction

$\text{Hg}_{1-x}\text{Mn}_x\text{Se}$ is a narrow-gap semiconductor with semi-magnetic properties [1] and a zinc blende crystal structure [2]. The optical and transport properties of these alloys are not yet sufficiently well known, unlike their semiconductor matrix HgSe [3, 4] and non-magnetic analogue $\text{Hg}_{1-x}\text{Cd}_x\text{Se}$ [5, 6].

From the Hall [7, 8] and Shubnikov–de Haas (sdH) [9, 10] experiments it has been determined that these alloys are usually of n-type conductivity. The intrinsic electron concentration is high ($n \approx 10^{17}–10^{18} \text{ cm}^{-3}$) and practically does not depend on the temperature. The electron mobility of these alloys is high (typical value at $T = 300 \text{ K}$ is $\mu \approx 10^4 \text{ cm}^2 \text{ V}^{-1} \text{ s}^{-1}$), and its temperature dependence is analogous to that of the non-magnetic semiconductor $\text{Hg}_{1-x}\text{Cd}_x\text{Se}$ (at higher temperatures it is determined primarily by electron scattering on the longitudinal optical phonons, and at lower temperatures mainly on the ionized defects) [6].

The $\text{Hg}_{1-x}\text{Mn}_x\text{Se}$ electron effective mass m^* on the Fermi surface, determined from the temperature dependence of the amplitude of magnetoresistance oscillations [9, 10], is small— $m^* = (3–7) \times 10^{-2} m_0$ (at 4.2 K).

Depending on its composition x , the $\text{Hg}_{1-x}\text{Mn}_x\text{Se}$ alloy becomes either a zero or narrow-gap semiconductor. At $T = 4 \text{ K}$, for $x < 0.06$ it is a semimetal, whereas for $x > 0.06$ it is a narrow-gap semiconductor [11].

The room-temperature far-infrared reflectivity measurements [12] show two-mode phonon behaviour in these alloys.

In this paper, the transport and optical properties of $\text{Hg}_{0.86}\text{Mn}_{0.14}\text{Se}$ single crystals are analysed by measuring the far-infrared (FIR) reflectivity spectra within the $50–350 \text{ cm}^{-1}$ spectral range, as well as the electrical resistivity, the Hall and sdH effects in magnetic fields from 0–6.5 T and in the temperature range from 4.2 to 300 K. The results of these measurements are the temperature dependences of the kinetic parameters of the crystal— $\tau(T)$, $n(T)$, $m^*(T)$, $\mu(T)$ —and the characteristic frequencies of plasmons and phonons.

2. Experimental procedure

The single crystal of $\text{Hg}_{0.86}\text{Mn}_{0.14}\text{Se}$ was grown by the modified Bridgman technique at the Institute of Physics of the Polish Academy of Sciences. The manganese concentration ($x = 0.14$) is determined by x-ray powder diffraction (XRPD) (the lattice parameter was found to be $a = 6.0567 \text{ \AA}$).

The sample for measuring transport properties was $4 \times 0.5 \times 0.5 \text{ mm}^3$, while the current and voltage contacts were up to 0.1 mm. The measurements were taken by the standard DC potentiometer method. The sample was supplied with current, usually up to 50 mA. A superconducting magnet of up to 6.5 T strength was the source of the magnetic field. The temperature of the sample was measured by a Cu/(Cu + 1% Fe) thermocouple.

The FIR reflectivity measurements were performed on a disc-shaped sample (diameter of 6 mm) using a Bruker IFS 113v spectrometer with an Oxford CF 100 cryostat.

3. Results and discussion

In figure 1, the FIR reflectivity spectra of $\text{Hg}_{0.86}\text{Mn}_{0.14}\text{Se}$ single crystals, within the $50\text{--}350\text{ cm}^{-1}$ range, are shown at several temperatures. The points are experimental data and curves are the spectra computed using the plasmon-phonon interaction model:

$$\varepsilon(\omega) = \varepsilon_{\infty} \left(\prod_{j=1}^3 \frac{\omega_{j\text{LO}}^2 - \omega^2 + i\gamma_{j2}\omega}{\omega_{j\text{TO}}^2 - \omega^2 + i\gamma_{j1}\omega} - \frac{\omega_p^2}{\omega(\omega + i\tau^{-1})} \right) \quad (1)$$

where ω_{TO} and ω_{LO} are the transverse and longitudinal frequencies, γ_1 and γ_2 are γ_{TO} dampings at ω_{TO} and ω_{LO} respectively, ω_p is the plasma frequency, τ is the free carrier relaxation time and ε_{∞} is the high-frequency dielectric constant. The first term in equation (1) is the lattice vibration contribution whereas the second term is the Drude expression for the free carrier contribution to the dielectric constant.

Here we used the model given by equation (1) because it decomposes the dielectric function into the sum of pure phonon (which has the advantage of describing the phonon reflectivity correctly) and pure plasmon contributions. The parameters used to fit infrared reflectivity data of $\text{Hg}_{0.86}\text{Mn}_{0.14}\text{Se}$ with equation (1) are given in table 1.

Three oscillators may be clearly observed at 104, 145 and 220 cm^{-1} in figure 1 (300 K). The first two are almost at the same frequencies as HgSe [14], identifying them as HgSe vibration modes. However, the 145 cm^{-1} mode is a HgSe zone centre, infrared, active optical mode whereas the 104 cm^{-1} mode is the result of a resonant two-phonon process [14]. This mode is almost routinely present in FIR reflectivity spectra of narrow gap semiconductors and those of their solid solutions [14, 15]. The 220 cm^{-1} mode is assigned as a MnSe zinc blende

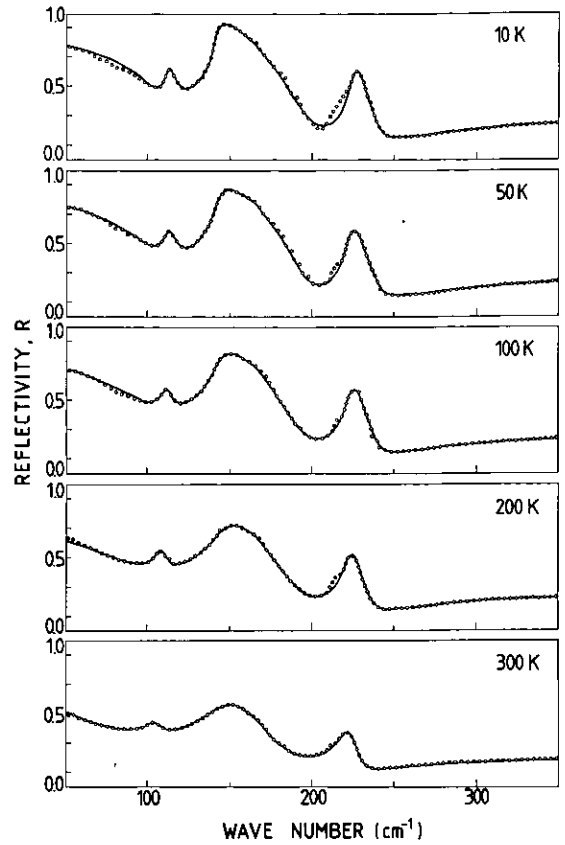


Figure 1. Far infrared reflectivity spectra of $\text{Hg}_{0.86}\text{Mn}_{0.14}\text{Se}$ at several temperatures. Experimental data are represented by open circles and the full curves are calculated spectra obtained by a fitting procedure based on the model described by equation (1) with parameter values given in table 1.

Table 1. Optical parameters of plasmons and phonons obtained by oscillator fitting of $\text{Hg}_{0.86}\text{Mn}_{0.14}\text{Se}$ reflection spectra.

Temperature (K)	ω_{TO} (cm^{-1})	γ_1 (cm^{-1})	ω_{LO} (cm^{-1})	γ_2 (cm^{-1})	ε_{∞}	ω_p (cm^{-1})	τ_0^{-1} (cm^{-1})	b (cm^2)
300	104	7.5	105.3	8	9.1	153	185.2	0
	145	23.5	169	24				
	219.5	10	225	9				
200	106.5	5	108	6	11.8	161	133.3	0.00013
	144	15.75	171.5	15.5				
	221	7.5	227.5	7.5				
100	110	5	111.5	5.6	12.8	172	101	0.00056
	142	9	169	7.5				
	222	7	229	6.75				
50	111.5	5.5	113.3	6.5	13	175	84.7	0.0006
	142.5	5.5	169	5				
	222	6	229	7				
10	112	4.5	113.75	5.6	13	182	76.9	0.00095
	141.5	3	168	1				
	224	5.5	230	5				

structure optical mode [12]. The detailed analysis of $\text{Hg}_{1-x}\text{Mn}_x\text{Se}$ vibrational properties was given in a previous paper [12].

By lowering the temperature, as shown in table 1, the frequencies of the observed modes at 104 and 220 cm^{-1} shift towards greater energies (mode hardening) while the frequency of 145 cm^{-1} mode decreases with the lowering of temperature (mode softening). It is worth mentioning here the increase of plasma frequency with decreasing temperature, which, as will be seen later, originates from the decreasing effective mass as a result of the temperature decrease.

At temperatures lower than room temperature, proper agreement between calculated and experimental spectra is obtained only by taking the frequency dependence of the free carrier relaxation time in the form of [16]:

$$\frac{1}{\tau} = \frac{1}{\tau_0} + b\omega^2. \quad (2)$$

The corresponding values for τ_0 and b are given in table 1.

Resistivity and Hall measurements at temperatures from 4.2 to 300 K are presented in figure 2. In the whole temperature range $\rho(T)$ is of metallic type. The Hall coefficient, which is $R_H = -32 \text{ cm}^3 \times \text{C}^{-1}$ at 4.2 K, practically does not depend on temperature. The coefficient R_H at 4.2 K does not depend on the magnetic field in the whole range in which measurements were taken (figure 3(a)).

From $R_H = 1/en$ the electron concentration $n = 1.9 \times 10^{17} \text{ cm}^{-3}$ at 4.2 K is determined. It does not depend on the temperature or the applied magnetic field, which suggests the absence of compensation in the examined crystal. By using the relation $\mu_H = R_H/\rho_0$ an electron mobility value of $\mu_H = 2600 \text{ cm}^2 \text{ V}^{-1} \text{ s}^{-1}$ at 4.2 K is determined.

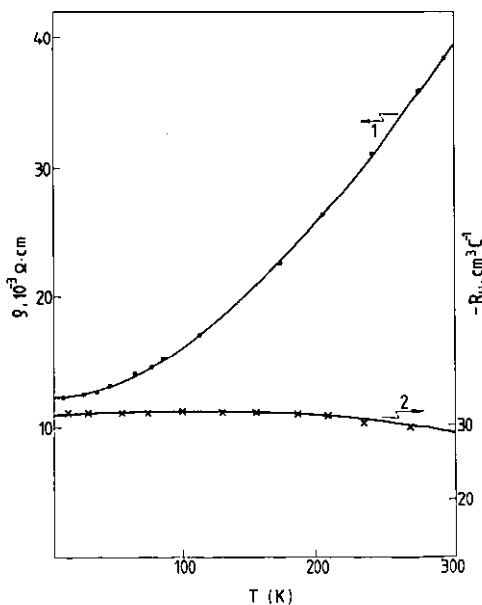


Figure 2. Resistivity (curve 1) and Hall coefficient (curve 2) of $\text{Hg}_{0.86}\text{Mn}_{0.14}\text{Se}$ against temperature.

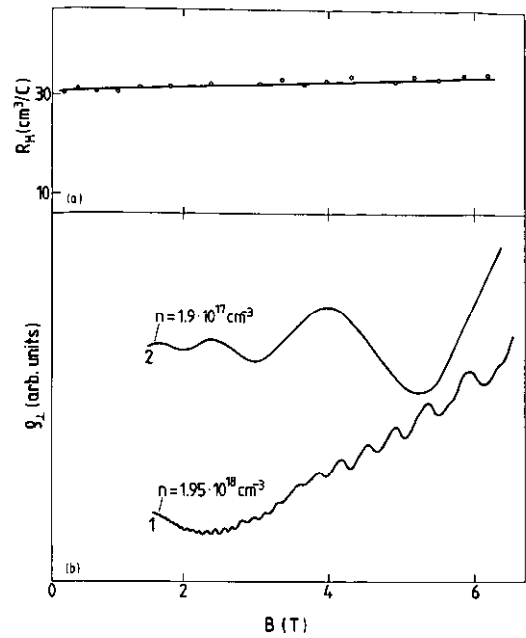


Figure 3. (a) Hall coefficient against magnetic field in $\text{Hg}_{0.86}\text{Mn}_{0.14}\text{Se}$ at 4.2 K. (b) Transverse magnetoresistance oscillations of $\text{Hg}_{1-x}\text{Mn}_x\text{Se}$ at 4.2 K. (curve 1, $x = 0.02$; curve 2, $x = 0.14$). Full line and curves are a guide to the eye.

The transverse magnetoresistance oscillations (sdH oscillations) of $\text{Hg}_{0.86}\text{Mn}_{0.14}\text{Se}$ at $T = 4.2 \text{ K}$ are shown in figure 3(b) (curve 2). For the sake of comparison, in the same figure the sdH oscillation curve of a sample with less Mn content ($x = 0.02$) is given. The non-monotonic dependence of the amplitude of sdH oscillations can be noticed, as well as a significant growth of the period of these oscillations with increasing content of the magnetic component (compare curves 1 and 2).

The sdH oscillations for a free electron system will be periodic in $1/B$ with the period [4]:

$$P_F = \frac{2e/hc}{(3\pi^2 n)^{2/3}}. \quad (3)$$

Using this relation and the oscillation dependence of $\rho_{\perp}(B)$ from figure 3 we obtained an electron concentration n_{SH} of $1.98 \times 10^{17} \text{ cm}^{-3}$. This value is in very good agreement with that obtained from the measurements of the Hall effect.

The temperature dependence of the effective electron mass m^* was determined by using the values of ω_p and ϵ_{∞} from table 1 as well as the relation $\omega_p^2 = ne^2/\epsilon_{\infty}m^*$. This dependence is shown in figure 4 (curve 1) where it can be seen that m^* increases with temperature in the range $T > 100 \text{ K}$, while in the low-temperature range the effective mass is nearly constant. At 10 K, $m^*/m_0 = 0.044$, which is in very good agreement with value $m^*/m_0 = 0.04$ which was obtained from the sdH effect for $\text{Hg}_{1-x}\text{Mn}_x\text{Se}$ with approximately the same electron concentration $n = 2 \times 10^{17} \text{ cm}^{-3}$ at $T = 11.3 \text{ K}$ [9].

In figure 4 (curve 2) the electron relaxation time τ is shown as a function of temperature. With an increase in temperature τ decreases from $0.71 \times 10^{-13} \text{ s}$ at 10 K to

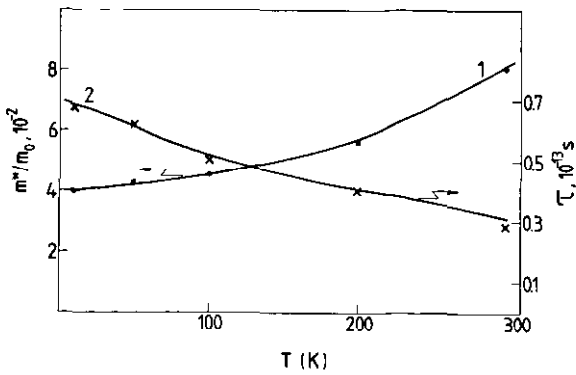


Figure 4. Temperature dependence of m^*/m_0 (curve 1) and of electron relaxation time τ (curve 2) of $\text{Hg}_{0.86}\text{Mn}_{0.14}\text{Se}$. Full curves are a guide to the eye.

0.34×10^{-13} s at 300 K. The relaxation time determined from the transport measurements (from the relation $\sigma = ne^2\tau/m^*$) changes in the same way with temperature (from 0.56×10^{-13} s at 10 K to 0.39×10^{-13} s at 300 K).

From $m^*(T)$ and $\tau(T)$ dependences, which have been obtained from optical measurements, and using the relation $\mu = e\tau/m^*$, the 'optical' electron mobility μ_{opt} was determined. The dependence $\mu_{\text{opt}}(T)$ is shown in figure 5 (broken curve) together with the same dependence obtained from the transport measurements (full curve) $\mu_{\text{H}}(T)$. The agreement between μ_{H} and μ_{opt} is very good in the temperature range $50 \text{ K} < T < 300 \text{ K}$. The discrepancy is noticeable at temperatures below 25 K. Thus, while μ_{H} tends to saturation (at 10 K, $\mu_{\text{H}} = \text{constant}$), μ_{opt} suddenly increases.

At a higher temperature ($T > 50 \text{ K}$), at which the dominant mechanism of scattering is on the longitudinal optical phonons, conformity of curves $\mu_{\text{opt}}(T)$ and $\mu_{\text{H}}(T)$ should be expected. Smaller discrepancies between values at 20 K and 30 K can be explained by the dominant scattering of electrons on the acoustic phonons. In the

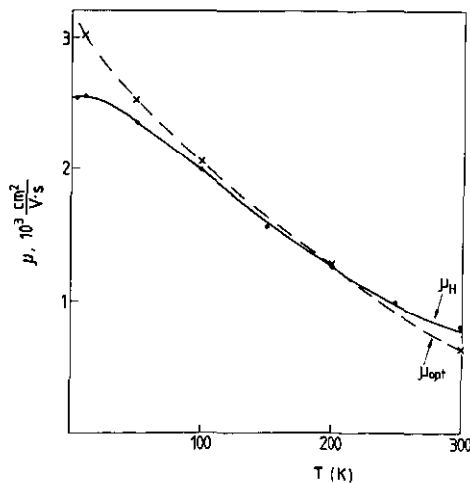


Figure 5. Temperature dependence of electron mobility obtained from optical μ_{opt} and Hall effect μ_{H} measurements. Full and broken curves are a guide to the eye.

range $T < 20 \text{ K}$, in which the mobility of electrons does not depend on the temperature, and the basic mechanism of relaxation of the carriers is scattering on the ionized impurities, the significant disagreement of the broken and full curves in figure 5 is quite understandable.

Scattering of the electrons on the magnetic moments of Mn ions in the $\text{Hg}_{0.86}\text{Mn}_{0.14}\text{Se}$ crystal has not been observed. According to Gavaleshko *et al* [18] it appears in these alloys when the content of manganese $x > 0.20$ and in the range of very low temperatures ($T < 4.2 \text{ K}$).

4. Conclusions

Transport (resistivity, Hall and sdlH) and optical (FIR reflectivity) measurements of $\text{Hg}_{0.86}\text{Mn}_{0.14}\text{Se}$ single crystal in the range 4.2–300 K, in magnetic fields up to 6.5 T have been performed.

The concentrations of electrons determined from Hall and sdlH effect measurements agree, $n_{\text{H}} \approx n_{\text{SH}} = 1.9 \times 10^{17} \text{ cm}^{-3}$. As is known, in $\text{Hg}_x\text{Mn}_{1-x}\text{Se}$, as well as in its semiconductor matrix HgSe, the extrinsic electrons originate from Hg atoms which are on interstitial sites, as well as from other stoichiometry defects of donor-type.

Acceptor centres in these alloys are vacancies in mercury sublattices and the acceptor impurity level is either in the conduction band (for $E_{\text{g}} < 0$) or in the band gap (for $E_{\text{g}} > 0$). The degree of the impurity level occupancy is defined by the ratio of the Fermi level and the band gap edge ($E_{\text{F}}/E_{\text{g}}$), as well as by the donor and acceptor concentration ratio ($N_{\text{d}}/N_{\text{a}}$) [18]. In the case when $N_{\text{d}} > N_{\text{a}}$ (low compensated semiconductor) the acceptor impurity level is completely occupied and has no influence on the transport properties. Our results ($\mu_{\text{H}} = \mu_{\text{SH}}$, as well as the independence of carrier concentration on both the temperature and the magnetic field) lead us to conclude that the examined crystal is a low compensated, degenerate semiconductor.

From the FIR reflectivity spectra of crystals which are numerically fitted by a model of plasmon-phonon interaction, the frequencies of phonons and plasmons and the temperature dependences of the effective mass and the electron relaxation time have been determined.

By comparison of $\mu_{\text{opt}}(T)$ with $\mu_{\text{H}}(T)$ it can be shown that these dependences are in good agreement at $T > 50 \text{ K}$. However, at $T < 50 \text{ K}$ scattering on ionized impurities is dominant so these dependences differ.

Acknowledgments

We thank Dr W Dobrowolski for the samples and W Konig for the measurement of the far-infrared spectra.

References

- [1] Brandt N B and Moshchalkov V V 1984 *Adv. Phys.* **33** 193
- [2] Pajaczowska A and Rabenau A 1977 *Mater. Res. Bull.* **12** 183

- [3] Lehoczky S L, Broerman J G, Nelson D A and Whitsett C R *Phys. Rev. B* **9** 1598
- [4] Whitsett C R 1965 *Phys. Rev.* **138** A829
- [5] Nelson A D, Broerman J G, Summers C J and Whitsett C R 1978 *Phys. Rev. B* **18** 1658
- [6] Iwanovski R J, Dietl T and Szymanska W 1978 *J. Phys. Chem. Solids* **39** 1059
- [7] Žižić O, Stojić M and Stošić B 1985 *Phys. Status Solidi a* **88** K191
- [8] Stošić B, Stojić M, Babić-Stojić B and Žižić O 1986 *Fizika* **18** 65
- [9] Takeyama S and Galazka R R 1979 *Phys. Status Solidi b* **96** 413
- [10] Lapilin I I, Ponomarev A I, Harus G I and Gavaleshko N P 1983 *Zh. Eksp. Teor. Fiz.* **85** 1639
- [11] Takeyama S and Galazka R 1979 *Phys. Status Solidi b* **96** 413
- [12] Čogurić G D, Popović Z V, Stojanović D, Žižić O and König W 1991 *Solid State Commun.* **17** 555
- [13] Baumard J F and Gervais F 1977 *Phys. Rev. B* **15** 2316
- [14] Witowski A and Grynberg M 1980 *Phys. Status Solidi b* **100** 389
- [15] Baars J and Sorger F 1972 *Solid State Commun.* **10** 875
- [16] Nagel S R and Schnatterly S E 1974 *Phys. Rev. B* **9** 1299
- [17] Kulbachinskii V A 1990 *Sov. Solid State Phys.* **32** 2493
- [18] Gavaleshko N P, Gorleij P N, Shenderovskij V A 1984 *Uskozonski Poluprovodniki Poluchenie i Fizicheskie Svoijstva* (Kiev: Akad. Nauk) p 160